Disentangling The Causes of Discrepancies In Simulated Immersion-mode Ice Nucleating Particles

Aishwarya Raman [1], Elise K. Wilbourn [2,3], Mikhail S. Pekour[1], Naruki Hiranuma [2], Susannah M. Burrows[1]

[1]Pacific Northwest National Lab, Richland, WA
[2]Dept. of Life, Earth and Environmental Sciences, West Texas A&M University,Canyon, TX
[3]*Now at Sandia National Laboratories,Livermore, CA

Key Points:

- Global climate model simulated immersion-mode INP concentrations are one to three orders of magnitude lower than INP measurements.
- Aerosol-INP closure is achieved (INPs within a factor of 10) for INPs simulated using the in situ aerosol measurements
- Errors in the model-simulated aerosol properties are the dominant cause of the model INP discrepancy .

Abstract

We assess the predictability of immersion-mode ice nucleating particles (INPs) at a remote marine site in the Eastern North Atlantic (ENA) using aerosol simulations from a global climate model as inputs to the immersion-mode INP parameterizations. While the model-simulated INP concentrations are lower by one to three orders of magnitudes compared to the measurements, we achieve aerosol-INP closure at ENA using the observed aerosol properties. We demonstrate a novel INP error decomposition approach to quantify the portion of total INP error from different error components. We conclude that inaccuracies in aerosols (surface area and composition) are the dominant cause of the model INP discrepancy at ENA. We recommend that, for future aerosol-INP closure studies, along with the measurements for total INP concentrations, campaigns should also collect co-located aerosol size-resolved composition measurements (in the INP-relevant size range) to better distinguish and quantify the error sources.

Plain Language Summary

We assess the predictability of ice nucleating particles (INPs) at a remote marine site in the Eastern North Atlantic (ENA) using aerosol simulations from a global climate model as inputs to the immersion-mode INP parameterizations. Model-simulated INP concentrations at ENA are lower by one to three orders of magnitude compared to the measurements. However, INPs predicted using the observed aerosol properties are within an order of magnitude from INP measurements. We quantify the portion of errors from aerosol and INP parameterization components. We conclude that inaccuracies in aerosol surface area and composition are the dominant causes for the model INP discrepancy at ENA.

1 Introduction

Mixed-phase clouds (MPCs) play a vital role in precipitation and radiation budget due to the presence of super-cooled liquid water and ice crystals (Korolev et al., 2017; Burrows et al., 2022). The dominant mechanism for heterogeneous ice formation in MPCs is the immersion-mode freezing of cloud droplets in the presence of ice nucleating particles (INPs) at temperatures warmer than $-38\,^{\circ}\mathrm{C}$ (Pruppacher et al., 1998; Vali et al., 2015). INPs are a rare subset of aerosols whose ice nucleating ability depends on the size-resolved particle composition, abundance, surface properties, and atmospheric conditions (e.g. DeMott et al., 2010; Boose et al., 2016).

In general, the INP number concentrations in the marine atmosphere are lower by an order of magnitude or more compared to those in terrestrial regions (e.g. DeMott et al., 2016). However, sea spray (salt + organics) emitted from bubble bursting in the ocean and mineral dust transported to the marine atmosphere from deserts can significantly affect the INP population in the marine boundary layer (e.g. Creamean et al., 2019; McCluskey et al., 2019). Previous studies over remote marine regions have shown that presence of INPs can alter climate feedbacks (e.g. Vergara-Temprado et al., 2018; Tan et al., 2022), but climate models can exhibit significant bias in prediction of INPs (Raman et al., 2022).

The predictive understanding of INPs in climate models is limited by sparse measurements of co-located aerosol size-resolved composition and INP number concentration. Recent INP studies have resorted to aerosol-INP closure experiments to investigate the error sources in INP prediction. Aerosol-INP closure for a given INP measurement temperature is defined as the agreement between the predicted INPs from observed aerosol properties and the measured INP concentrations within measurement uncertainties (Burrows et al., 2022). Knopf et al. (2021) conducted aerosol-INP closure during a frontal passage at the Department of Energy (DOE) site in the Southern Great Plains, and found that size-resolved INP com-

position and individual INP propensity are especially important for closure in regions with frequent variations in meteorological and aerosol conditions.

In this study, we assess the dominant cause of errors in the boundary-layer immersion-mode INP predictability during the DOE field campaign, Examining the Ice Nucleating Particles from the Eastern North Atlantic (ExINP-ENA), from October 2020 to December 2020 (Hiranuma et al., 2022). We perform aerosol-INP closure at ENA (39.09°N, 28.02°W) (Text S1) and constrain the spread in modeled INP concentrations using different aerosol measurements and INP parameterizations. We introduce a novel error decomposition approach to quantify the portion of total INP discrepancy between model and observations associated with individual error sources. We illustrate the methods for the aerosol-INP closure and INP error decomposition in Section 2, describe and discuss our findings in Section 3 and Section 4.

2 Methods

2.1 Aerosol and INP Measurements

We summarize the suite of aerosol and INP measurements in Table S1. We estimate the total aerosol surface area per unit volume (S_{aer} [$m^2\,m^{-3}$]) and related uncertainties using the ARM Aerosol Observing System (AOS) nephelometer-based aerosol scattering efficiency measurements (DeMott et al., 2016; Testa et al., 2021) at 450 nm wavelength (Text S3). We calculate six hourly averages of S_{aer} estimates to match time stamps in the INP measurements. For particle-type classification, we use the elemental composition data (based on 100 particle samples) from scanning electron microscopy coupled with energy-dispersive X-ray spectroscopy (SEM-EDX) (China et al., 2017). We estimate the total atomic weight proportion for dust and sea spray particles using the classification techniques in Cheng et al. (2016) and Hiranuma et al. (2013) (Text S4 and Table S2).

We use immersion mode ambient INP number concentrations measured with the Portable Ice Nucleation Experiment (PINE) chamber (Bilfinger Noel, model PINE-3) (Möhler et al., 2021) at temperatures between $-14\,°C$ and $-33\,°C$. INP concentrations were measured approximately every 12 minutes, and measurements were averaged for six hours to obtain adequate sampling statistics in a clean marine environment. We derive temperature-dependent errors for INP concentrations (Hiranuma et al., 2022) in terms of a 95% confidence interval (CI) using the Poisson statistics (Krishnamoorthy & Lee, 2013) (Text S6).

2.2 Model Overview and INP Parameterizations

We use the U.S. DOE Energy Exascale Earth System Atmosphere Model version 1 (EAMv1) (Neale et al., 2010; Golaz et al., 2022) with the modal aerosol module with four log-normal modes (MAM4) (H. Wang et al., 2020) to simulate the size-resolved aerosol composition inputs for the INP parameterizations. We provide more details about the EAMv1 model in Text S7.

We quantify the IN efficiency ($n_s(T)$ [INP concentrations per unit area, m^{-2}]) for dust and sea spray INPs using the temperature-dependent ice nucleation active site (INAS) parameterizations (Table S3). We derive INP concentrations by multiplying the $n_s(T)$ estimates with dust/sea spray surface area, depending on the INP type.

We include only dust and sea spray INPs at ENA because these two aerosol types have been commonly observed at ENA in previous studies (Y. Wang et al., 2020; Zheng et al., 2018). We estimate sea spray $n_s(T)$ following McCluskey et al. (2018). For dust INPs, we use multiple $n_s(T)$ parameterizations: Boose et al. (2016) (B16 Morocco, B16 Pelopennese),

Ullrich et al. (2017) (UL17), and Reicher et al. (2019) (REI19 super-micron) (Text S8 and Text S9).

2.3 Experiment Design and INP Closure

We ran EAMv1 simulations for the period of January-December 2020 with approximately 100 km horizontal resolution and 72 vertical layers using prescribed sea surface temperature and constrained meteorology (S. Zhang et al., 2022). We nudged the model winds at all model vertical levels using the Modern-Era Retrospective Analysis for Research and Applications, version 2 (MERRA-2) reanalysis data (Gelaro et al., 2017) at a 6-h relaxation time scale.

To permit spatial and temporal co-location between model outputs and INP measurements, we use the simulated aerosol fields at the nearest model grid box to the ENA station and use the 6-hourly averaged model outputs to estimate INP concentrations. We calculate the INP concentrations offline (i.e. model cloud microphysics is not affected by the INPs simulated in this study) by using the EAMv1-simulated and co-located dust and sea spray aerosols and the INP parameterizations.

We characterize the INP discrepancy between EAMv1-predicted INPs and PINE measurements in terms of modified normalized bias (MNB) (Equation 1), which is calculated as the difference in two quantities divided by the sum of the quantities (Text S10). Equation 1 shows a general formula for estimating MNB from two INP calculations, $\mathrm{INP}_1(T)$ and $\mathrm{INP}_2(T)$.

$$\mathrm{MNB}\left(\mathrm{INP}_1(T), \mathrm{INP}_2(T)\right) = \frac{\mathrm{INP}_1(T) - \mathrm{INP}_2(T)}{\mathrm{INP}_1(T) + \mathrm{INP}_2(T)}\,. \tag{1}$$

To quantify the aerosol-INP closure (schema in Figure S3), we estimate INP concentrations using the observed aerosol properties ('closure INPs'), nephelometer-estimated S_{aer} and the SEM-EDX derived fraction of dust and sea spray in the total chemical composition for 100 SEM-EDX samples. We declare aerosol-INP closure if the closure INP estimates are within a factor of 10 from the measurements. We express the closure error using the MNB metric.

Several climate modeling studies in the literature have adopted error decomposition techniques to determine the dominant processes contributing to bias in GCM simulated feedbacks (e.g. Tian et al., 2009; Y. Zhang et al., 2021; Zelinka et al., 2016). For a given INP measurement temperature, we express the total predicted INP discrepancy (E_p) as a linear combination of three error sources: the portion of E_p associated with S_{aer} ($E_{S_{aer}}$), composition (E_c), and residual sources (E_{res}) (Equation 2). Finally, we quantify the uncertainty in each error source given the independent aerosol and INP measurements, each with an uncertainty (Table 2). We use an uncertainty propagation technique to quantify the uncertainties in E_c and E_{res} (Text S11).

$$E_{\mathrm{p}} = E_{\mathrm{Saer}} + E_{\mathrm{c}} + E_{\mathrm{res}}\,. \tag{2}$$

3 Results

3.1 Comparing Simulated and Observed Aerosol Properties

Figure 1 compares the co-located surface level dust (Figure 1a), sea spray (Figure 1b), and total surface area (Figure 1c) from EAMv1 simulations and in situ measurements at ENA.

Experiment name	**Surface area**	**Aerosol composition**
INP E3SM	S_{aer} from E3SM for the size range $0.08 - 10\mu m$	E3SMv1 simulations of dust and sea spray aerosol fractions
INP E3SM NEPH	Dust and sea spray aerosol surface were calculated using S_{aer} from the AOS nephelometer	E3SMv1 simulations of dust and sea spray aerosol fractions
INP EDX E3SM	S_{aer} from E3SMv1	Aerosol fraction for dust and sea spray from SEM-EDX
INP EDX NEPH	S_{aer} from the nephelometer	Aerosol fraction for dust and sea spray from SEM-EDX

Table 1. INP calculations using various observed and simulated aerosol quantities.

Overall, the EAMv1-simulated surface area estimates are typically lower by one to two orders of magnitude compared to the in situ measurements. For the particle-type fraction, EAMv1 overestimates sea spray fraction and underestimates dust fraction compared to SEM-EDX measurements, both approximately by an order of magnitude. To better understand the aerosol classification at ENA, we compare our SEM-EDX classification with Knopf et al., 2022 analysis at the ENA site (Text S5).

The biases in EAMv1-simulated aerosols over the remote marine regions are mainly due to the high vertical resolution and higher dry deposition rates in the model (a factor of two compared to CAM5 and other AeroCom (Aerosol Comparisons Observations and Models) models) (Wu et al., 2020; Feng et al., 2022). Such biases in dry deposition velocities are not uncommon to global models (e.g. Emerson et al., 2020). In addition to dry deposition, aerosol biases in EAMv1 are also affected by biases in other physical processes such as aerosol wet scavenging (K. Zhang et al., 2022). In marine regions where INP concentrations are already lower compared to continental regions, systematic differences between the simulated and observed aerosol surface area and composition as large as two orders of magnitude will directly affect the magnitude of INPs estimated using the simulated aerosol quantities.

3.2 INP Concentrations at ENA

Figure 2 compares the 6-hourly averaged INP number concentration measurements from PINE with EAMv1-simulated (and co-located) dust and sea spray INP concentrations for different measurement temperatures. The lack of strong seasonal variability in the INP measurements at ENA suggests that dust and sea spray INPs are persistent INP sources throughout the year. The INP number concentration measurements over the study period range from $0.1\,\mathrm{L}^{-1}$ to $100\,\mathrm{L}^{-1}$ for temperatures between $-20\,^{\circ}\mathrm{C}$ and $-30\,^{\circ}\mathrm{C}$ respectively. However, INP E3SM estimates (Blue lines in Figure 2) are generally lower by one to two orders of magnitudes compared to the INP measurements. We find that combining EAMv1-simulated sea spray (M18) and dust INPs provides little improvement in the model-observation discrepancy at ENA.

Among the dust INP parameterizations (Table S3), UL17, B16 Pelopennese, and B16 Morocco show the maximum, median, and minimum discrepancies with measurements, respectively. Higher INP concentrations in B16 Morocco are likely due to the higher IN propensity of milled dust samples used for the development of the parameterization (Boose et al., 2016). Milling increases the surface irregularities, which in turn increases the IN activity (Reicher et al., 2019). Given these caveats about the IN efficiency of milled dust samples, it is possible that the good agreement between simulated B16 Morocco INPs and PINE measurements at ENA is likely due to the compensating errors between dust surface area underestimation in EAMv1 and $n_s(T)$ overestimation in B16 Morocco.

Error source / Calculation	**Purpose**	**Uncertainty calculation**
$E_p = \mathrm{MNB}(\mathrm{INP}_{\mathrm{E3SM}}, \mathrm{INP}_{\mathrm{OBS}})$	Total predictive skill error for E3SM v1 simulated vs. observed INP concentrations	Associated with different dust INP parameterizations.
$E_{S_{\mathrm{aer}}} = \mathrm{MNB}(\mathrm{INP}_{\mathrm{E3SM}}, \mathrm{INP}_{\mathrm{E3SM\ NEPH}})$	Portion of E_p associated with mismatch in simulated and observed S_{aer}	Calculated using uncertainties in the nephelometer scattering coefficients, Q (lower bound = 0.42, upper bound = 3.0).
$E_{\mathrm{c}} = \mathrm{MNB}(\mathrm{INP}_{\mathrm{E3SM\ NEPH}}, \mathrm{INP}_{\mathrm{EDX\ NEPH}})$	Portion of $E_{S_{aer}}$ associated with mismatch in E3SMv1 simulated vs. observed aerosol composition.	Calculated by propagating standard errors in SEM-EDX aerosol fraction to MNMB. For E3SM NEPH, we use a median Q = 2.0.
$E_{\mathrm{res}} = \mathrm{MNB}(\mathrm{INP}_{\mathrm{EDX\ NEPH}}, \mathrm{INP}_{\mathrm{OBS}})$	Residual errors (e.g., missing INP sources, errors in INP parameterizations, and atmospheric transformation of INPs.)	Calculated by propagating temperature dependent errors in measurements to MNMB. We use a median dust and sea spray fraction from EDX.

Table 2. INP error decomposition and uncertainty calculation for individual error components

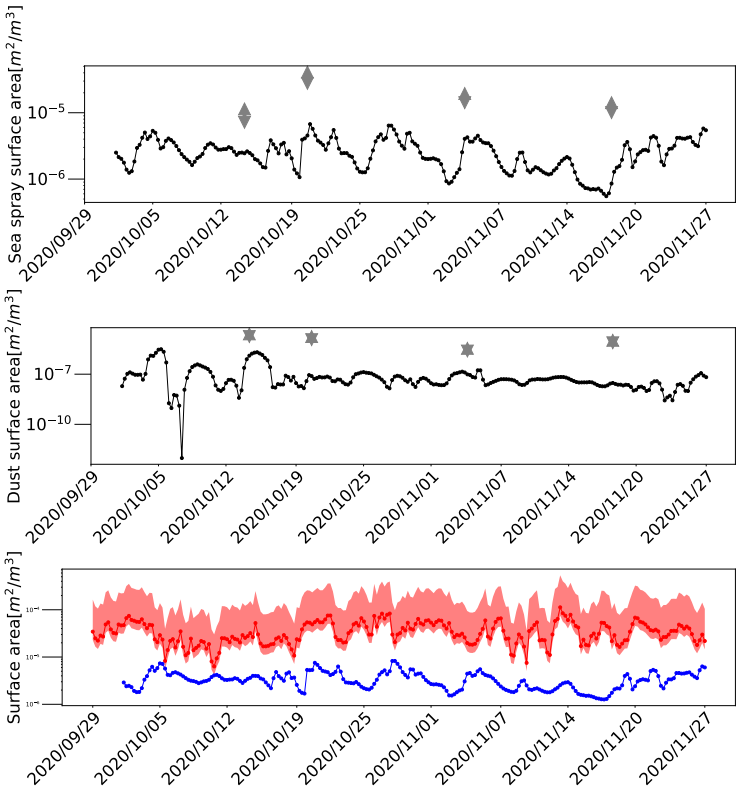

Figure 1. (a) Simulated (black) and observed (grey) dust surface area from E3SMv1 simulations and SEM-EDX (dust fraction) + Nephelometer (total surface area), respectively, along with the measurement uncertainties. (b) Same as (a) but comparing observations and model for sea spray aerosol surface area. (c) Simulated (blue) and observed (red) total surface area from E3SMv1 and the Nephelometer, respectively, along with the Nephelometer surface area uncertainties (red shaded region) calculated using the upper (3.0) and lower (0.42) bound for assumptions of scattering coefficients. Surface area estimates shown here for EAMv1 cover the size range 80 nm to 10 µm. In panels (a) and (b), observed surface area for dust and sea spray was estimated using the SEM-EDX particle-type classification. Each SEM-EDX measurement represents a sampling period of two to three days. To calculate the dust and sea spray surface area using the SEM-EDX particle-type classification data, we used the total surface area from the Nephelometer corresponding to the last day of the SEM-EDX measurement.

Overall, the uncertainty in the model discrepancies for different INP parameterizations is in the same order of magnitude as the discrepancy due to the simulated aerosol properties (Figure 2, blue and red lines). This leads to the next question, what is the dominant cause of the model INP discrepancies at ENA - aerosol errors or deficiencies in the INP parameterizations?

3.3 INP Closure, Error Decomposition, and Uncertainty Propagation

Figure 2 compares the closure INPs (green squares) predicted using the observed aerosol properties against the EAMv1-simulated (blue) and measured (black) INP concentrations. We find that adding sea spray and dust INPs does not reduce the closure. The closure INPs (Figure 2, green squares) are within an order of magnitude from the PINE measurements, the criterion we use in this study for aerosol-INP closure. These results confirm that the

[ht]

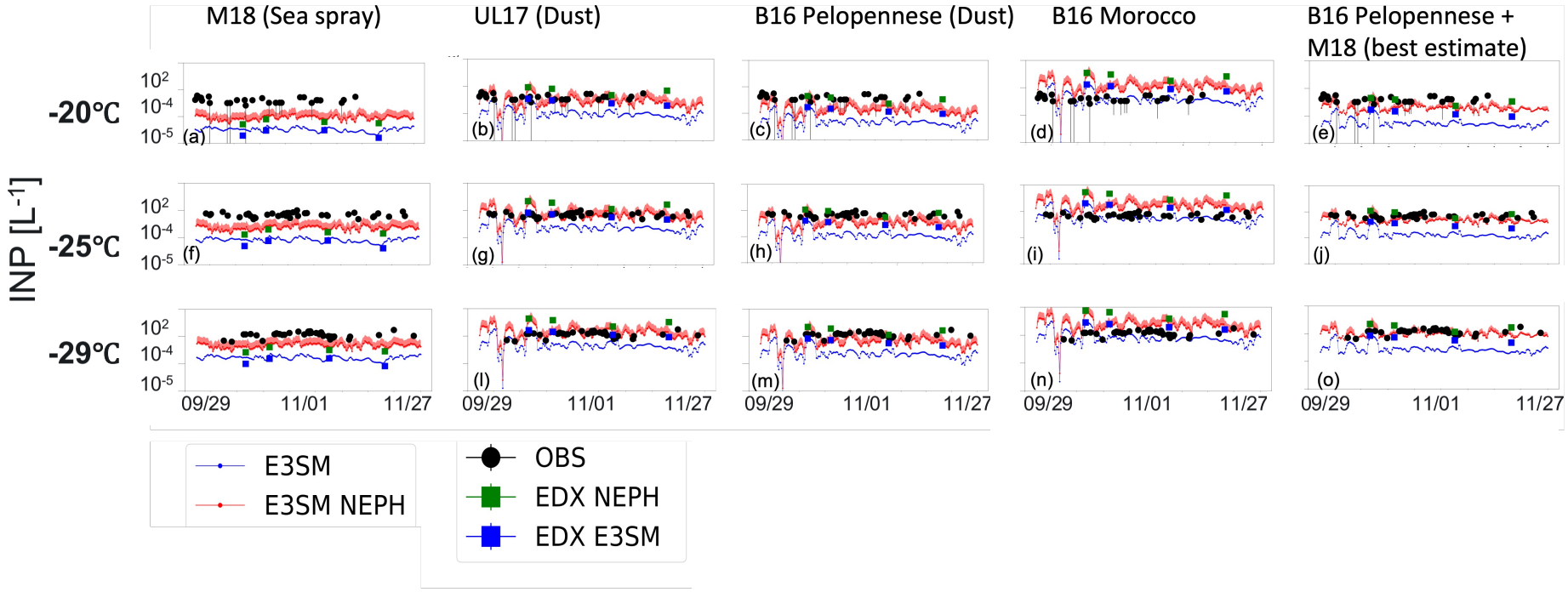

Figure 2. Time series of observed and modeled INP concentrations at −20°C,−25°C and −29°C. INP concentrations from PINE observations (ENA OBS) are shown as black circles. Different INP calculations are listed in Table 1.

EAMv1-simulated INP discrepancies as high as two to three orders of magnitude cannot be explained only by the deficiencies in the INP parameterizations.

Figure 3 illustrates the decomposition of model INP discrepancies (E_p) into error components associated with the simulated surface area ($E_{S_{aer}}$), composition (E_c), and the residual sources (closure error) (E_{res}). We find that $E_{S_{aer}}$+ E_c together estimate 20-30% higher median MNB compared to the MNB for E_{res}. The opposite signs for E_{res} and aerosol components ($E_{S_{aer}}$ and E_c) indicate that these two error sources partially compensate for one another. Therefore, improving only the INP parameterization errors without improving the aerosol errors in the model simulations will result in compensating biases in the model-predicted INPs.

We conclude that the inaccuracies in aerosol surface area and composition simulated in EAMv1 are the major reasons for the large discrepancy in model-predicted INP concentrations during the ExINP-ENA campaign. Along with improving the representation of aerosol properties in the model, accounting for deficiencies in the INP parameterizations by including missing INP sources and INP chemistry (e.g. biological INPs, coating of dust by sulfuric acid (Huang et al., 2021; Sullivan et al., 2010)) can further improve the INP closure at ENA.

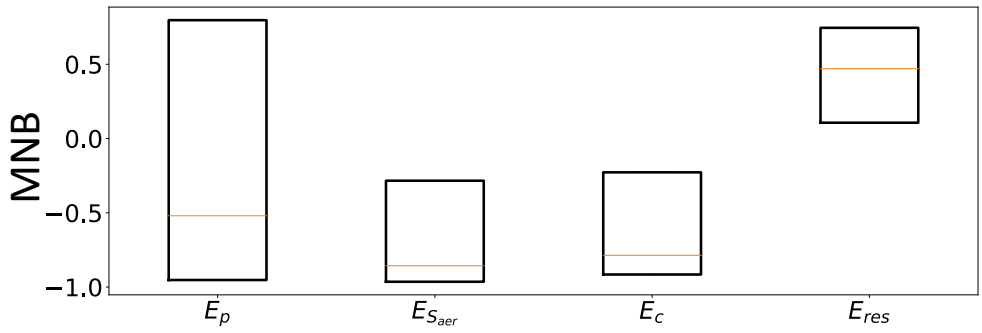

Figure 3. Decomposition of total INP discrepancies (dust and sea spray) at −29°C into individual error components, $E_{S_{aer}}$, E_c, and E_{res}. Table 2 describes the error components and uncertainties. The uncertainties in E_p are from using different dust INP parameterizations. For other error components, we show results only for the B16 Peloponnese + M18 INPs which have the least closure error compared to other dust parameterizations. Different nephelometer surface area estimates are derived based on the uncertainties in the scattering coefficient assumptions. The MNB range in $E_{S_{aer}}$ corresponds to using the lower and upper bound for nephelometer-derived surface area estimates in the INP parameterizations. Due to the limited number of temporally coincident observations from EDX, Neph, and PINE, sampling days for error sources are not the same. The number of days used for the calculation of E_p and $E_{S_{aer}}$ and their associated uncertainties are: 238 and 226. E_c and E_{res} represent four coincident SEM-EDX and INP samples. Upper and lower bounds for E_c are calculated using the variability in EDX errors in dust and sea spray fractions for different days during the campaign. We calculate E_{res} only for −29°C because of the limited availability of coincident measurements for SEM-EDX particle-type classification, PINE INP measurements, and temperature-dependent INP measurement errors at this temperature.

4 Discussion and Conclusion

In this study, we have investigated the predictive capability of EAMv1 and INAS-based INP parameterizations to simulate immersion-mode INP concentrations during the ExINPENA campaign at ENA, with an eye towards determining the leading cause of model-observation INP discrepancies. The EAMv1-simulated INP concentrations are one to three orders of magnitude lower than the INP measurements from PINE. We achieve INP closure (INP discrepancy within a factor of 10) when INPs are predicted using the measured aerosol properties from the AOS nephelometer and SEM-EDX. This evidence confirms that we cannot reduce such large discrepancies in the predicted INPs only by resolving the flaws in the INP parameterizations, but it is important to accurately represent the aerosol properties in the model to improve INP predictions.

We have demonstrated a novel INP error decomposition to quantify the portion of total INP model-observation discrepancies from different error sources. At the ENA site, we find that the inaccuracy in the EAMv1-simulated aerosol properties is the leading cause for the model INP discrepancies. Therefore, we conclude that correctly simulating the aerosol physical and chemical processes in the model is critical for accurately predicting the immersion-mode INP concentrations at ENA.

We note below some caveats of this study and their implications for the results. We used EAMv1-simulated aerosols for particle size range from 80 nm to 10 µm, whereas, PINE INP measurements are sensitive only up to 3 µm. Additionally, SEM-EDX size distribution data for ENA (for 100 samples) showed that only 10 to 17% of the surface area is between 3 µm and 5 µm. Therefore, almost an order of magnitude difference between the observed and simulated INPs cannot be attributed predominantly to the differences in the size cut off between PINE and the nephelometer.

We demonstrated the INP error decomposition method only for $-29\,^{\circ}\mathrm{C}$, because we did not have co-located SEM-EDX and INP measurements for other temperatures. Although we have considered only the temperature-dependent errors associated with counting statistics in the closure calculations, we recognize that other systematic uncertainties (e.g. loss of larger ice crystals between the PINE chamber and the optical counter, overlap in the size distribution of smaller ice crystals with the larger particles not activated to droplets) can also affect the INP measurements. Möhler et al. (2021) showed that for immersion freezing of mineral dust aerosols, PINE INP measurements were within the experimental uncertainties (%20) of the INP measurements from the Aerosol Interaction and Dynamics in the Atmosphere cloud chamber experiments.

Despite these caveats, this study provides key insights into the dominant sources of errors in immersion-mode INPs in the EAMv1 climate model. The INP error decomposition method we have demonstrated here can be modified and applied to other regions and field experiments. The information gained from the decomposition enables us to make recommendations for both model development and future field campaigns.

Improving INPs in climate models can significantly impact the simulated super-cooled liquid water (SLW) in MPC clouds, albedo, and climate. For example, a global climate modeling study found that with fewer INPs, the negative cloud-phase feedback was weakened, and strongly impacting the sea ice loss and Arctic Amplication (Tan et al., 2022). Overall, by better diagnosing and reducing the causes of INP errors, we can improve confidence in the use of aerosol-aware INP parameterizations in climate models and consequently reduce uncertainites in climate predictions (Burrows et al., 2022).

Acknowledgments

A. Raman thanks Catherine L. Himes from the PNNL communication team for technical editing support. A. Raman and S.M. Burrows were funded by the U.S. Department of Energy (DOE), Office of Science, Office of Biological and Environmental Research through the Early Career Research Program. N.Hiranuma and E.K.Wilbourn were funded under the DOE grant DE-SC-0018979. The Pacific Northwest National Laboratory is operated for DOE by Battelle Memorial Institute under contract DE-1713 AC05-76RL01830. E. K. Wilbourn and High-performance computing resources for this project was provided by the PNNL Research Computing, and the National Energy Research Scientific Computing Center (NERSC), a DOE Office of Science User Facility supported by the Office of Science of the U.S. Department of Energy under Contract No. DE-AC02-05CH11231.

Data Availability Statement E3SMv1 model simulated and co-located aerosol and INP data at ENA, SEM-EDX observations, nephelometer-based surface area estimates, and the corresponding Python scripts used for the analysis are available in the Zenodo repository DOI:10.5281/zenodo.7746607. PINE INP observations are archived in the ARM repository `https://www.arm.gov/research/campaigns/ena2020exinpena`. Aerosol scattering measurements from the Nephelometer are available in the ARM archive `https://adc.arm.gov/discovery/#/results/s::nephelometer`

Supporting Information ENAGRLSIworking.pdf

References

Boose, Y., Welti, A., Atkinson, J., Ramelli, F., Danielczok, A., Bingemer, H. G., ... Lohmann, U. (2016). Heterogeneous ice nucleation on dust particles sourced from nine deserts worldwide–part 1: Immersion freezing. *Atmospheric Chemistry and Physics*, *16*(23), 15075–15095.

Burrows, S. M., McCluskey, C. S., Cornwell, G., Steinke, I., Zhang, Kai, ... others (2022). Ice-nucleating particles that impact clouds and climate: Observational and modeling research needs. *Reviews of Geophysics*, e2021RG000745.

Cheng, C.-L., Chang, H.-H., Chen, T.-H., Tsai, P.-J., Huang, Y.-T., Huang, P.-J., & Lin, S.-Y. (2016). Spectral and morphological classification of different chronic and acute taiwanese gallstones via ftir, sem and esem-edx microanalyses. *Digestive and Liver Disease*, *48*(5), 519–527.

China, S., Alpert, P. A., Zhang, B., Schum, S., Dzepina, K., Wright, K., ... others (2017). Ice cloud formation potential by free tropospheric particles from long-range transport over the northern atlantic ocean. *Journal of Geophysical Research: Atmospheres*, *122*(5), 3065–3079.

Creamean, J., Cross, J. N., Pickart, R., McRaven, L., Lin, P., Pacini, A., ... others (2019). Ice nucleating particles carried from below a phytoplankton bloom to the arctic atmosphere. *Geophysical Research Letters*, *46*(14), 8572–8581.

DeMott, P. J., Hill, T. C., McCluskey, C. S., Prather, K. A., Collins, D. B., Sullivan, R. C., ... others (2016). Sea spray aerosol as a unique source of ice nucleating particles. *Proceedings of the National Academy of Sciences*, *113*(21), 5797–5803.

DeMott, P. J., Prenni, A. J., Liu, X., Kreidenweis, S. M., Petters, M. D., Twohy, C. H., ... Rogers, D. (2010). Predicting global atmospheric ice nuclei distributions and their impacts on climate. *Proceedings of the National Academy of Sciences*, *107*(25), 11217–11222.

Emerson, E. W., Hodshire, A. L., DeBolt, H. M., Bilsback, K. R., Pierce, J. R., McMeeking, G. R., & Farmer, D. K. (2020). Revisiting particle dry deposition and its role in radiative effect estimates. *Proceedings of the National Academy of Sciences*, *117*(42), 26076–26082.

Feng, Y., Wang, H., Rasch, P., Zhang, K., Lin, W., Tang, Q., ... Yu, H. (2022). Global dust cycle and direct radiative effect in e3sm version 1: Impact of increasing model resolution. *Journal of Advances in Modeling Earth Systems*, *14*(7), e2021MS002909.

Gelaro, R., McCarty, W., Suárez, M. J., Todling, R., Molod, A., Takacs, L., ... others (2017). The modern-era retrospective analysis for research and applications, version 2 (merra-2). *Journal of climate*, *30*(14), 5419–5454.

Golaz, J.-C., Van Roekel, L. P., Zheng, X., Roberts, A. F., Wolfe, J. D., Lin, W., ... others (2022). The doe e3sm model version 2: overview of the physical model and initial model evaluation. *Journal of Advances in Modeling Earth Systems*, *14*(12).

Hiranuma, N., Brooks, S. D., Moffet, R. C., Glen, A., Laskin, A., Gilles, M. K., ... McFarquhar, G. (2013). Chemical characterization of individual particles and residuals of cloud droplets and ice crystals collected on board research aircraft in the isdac 2008 study. *Journal of Geophysical Research: Atmospheres*, *118*(12), 6564–6579.

Hiranuma, N., Wilbourn, E. K., & Lacher, L. (2022). *Examining the ice-nucleating particles from the eastern north atlantic (exinp-ena) field campaign report* (Tech. Rep.). Oak Ridge National Lab.(ORNL), Oak Ridge, TN (United States). Atmospheric ....

Huang, S., Hu, W., Chen, J., Wu, Z., Zhang, D., & Fu, P. (2021). Overview of biological ice nucleating particles in the atmosphere. *Environment International*, *146*, 106197.

Knopf, D. A., Barry, K., Brubaker, T., Jahl, L., Jankowski, K., Li, J., ... others (2021). Aerosol–ice formation closure: A southern great plains field campaign. *Bulletin of the American Meteorological Society*, *102*(10), E1952–E1971.

Korolev, A., McFarquhar, G., Field, P. R., Franklin, C., Lawson, P., Wang, Z., ... others (2017). Mixed-phase clouds: Progress and challenges. *Meteorological Monographs*, *58*, 5–1.

Krishnamoorthy, K., & Lee, M. (2013). New approximate confidence intervals for the difference between two poisson means and comparison. *Journal of Statistical Computation and Simulation*, *83*(12), 2232–2243.

McCluskey, C. S., DeMott, P. J., Ma, P.-L., & Burrows, S. M. (2019). Numerical representations of marine ice-nucleating particles in remote marine environments evaluated against observations. *Geophysical Research Letters*, *46*(13), 7838–7847.

McCluskey, C. S., Hill, T. C., Sultana, C. M., Laskina, O., Trueblood, J., Santander, M. V., ... others (2018). A mesocosm double feature: Insights into the chemical makeup of marine ice nucleating particles. *Journal of the Atmospheric Sciences*, *75*(7), 2405–2423.

Möhler, O., Adams, M., Lacher, L., Vogel, F., Nadolny, J., Ullrich, R., ... others (2021). The portable ice nucleation experiment (pine): a new online instrument for laboratory studies and automated long-term field observations of ice-nucleating particles. *Atmospheric Measurement Techniques*, *14*(2), 1143–1166.

Neale, R. B., Chen, C.-C., Gettelman, A., Lauritzen, P. H., Park, S., Williamson, D. L., ... others (2010). Description of the ncar community atmosphere model (cam 5.0). *NCAR Tech. Note NCAR/TN-486+ STR*, *1*(1), 1–12.

Pruppacher, H. R., Klett, J. D., & Wang, P. K. (1998). *Microphysics of clouds and precipitation.* Taylor & Francis.

Raman, A., Hill, T., DeMott, P., Singh, B., Zhang, K., Ma, P.-L., ... Burrows, S. (2022). Long-term variability in immersion-mode marine ice nucleating particles from climate model simulations and observations. *Atmospheric Chemistry and Physics Discussions*, 1–36.

Reicher, N., Budke, C., Eickhoff, L., Raveh-Rubin, S., Kaplan-Ashiri, I., Koop, T., & Rudich, Y. (2019). Size-dependent ice nucleation by airborne particles during dust events in the eastern mediterranean. *Atmospheric Chemistry and Physics*, *19*(17), 11143–11158.

Sullivan, R., Petters, M. D., DeMott, P. J., Kreidenweis, S. M., Wex, H., Niedermeier, D., ... others (2010). Irreversible loss of ice nucleation active sites in mineral dust particles caused by sulphuric acid condensation. *Atmospheric Chemistry and Physics*, *10*(23), 11471–11487.

Tan, I., Barahona, D., & Coopman, Q. (2022). Potential link between ice nucleation and climate model spread in arctic amplification. *Geophysical Research Letters*, *49*(4), e2021GL097373.

Testa, B., Hill, T. C., Marsden, N. A., Barry, K. R., Hume, C. C., Bian, Q., ... others (2021). Ice nucleating particle connections to regional argentinian land surface emissions and weather during the cloud, aerosol, and complex terrain interactions experiment. *Journal of Geophysical Research: Atmospheres*, *126*(23), e2021JD035186.

Tian, Y., Peters-Lidard, C. D., Eylander, J. B., Joyce, R. J., Huffman, G. J., Adler, R. F., ... Zeng, J. (2009). Component analysis of errors in satellite-based precipitation estimates. *Journal of Geophysical Research: Atmospheres*, *114*(D24).

Ullrich, R., Hoose, C., Möhler, O., Niemand, M., Wagner, R., Höhler, K., ... Leisner, T. (2017). A new ice nucleation active site parameterization for desert dust and soot. *Journal of the Atmospheric Sciences*, *74*(3), 699–717.

Vali, G., DeMott, P., Möhler, O., & Whale, T. (2015). A proposal for ice nucleation terminology. *Atmospheric Chemistry and Physics*, *15*(18), 10263–10270.

Vergara-Temprado, J., Miltenberger, A. K., Furtado, K., Grosvenor, D. P., Shipway, B. J., Hill, A. A., ... Carslaw, K. S. (2018). Strong control of southern ocean cloud reflectivity by ice-nucleating particles. *Proceedings of the National Academy of Sciences*, *115*(11), 2687–2692.

Wang, H., Easter, R., Zhang, R., Ma, P.-L., Singh, B., Zhang, K., ... others (2020). Aerosols in the e3sm version 1: New developments and their impacts on radiative forcing. *Journal of Advances in Modeling Earth Systems*, *12*(1), e2019MS001851.

Wang, Y., Zheng, X., Dong, X., Xi, B., Wu, P., Logan, T., & Yung, Y. L. (2020). Impacts of long-range transport of aerosols on marine-boundary-layer clouds in the eastern north atlantic. *Atmospheric Chemistry and Physics*, *20*(23), 14741–14755.

Wu, M., Liu, X., Yu, H., Wang, H., Shi, Y., Yang, K., ... others (2020). Understanding processes that control dust spatial distributions with global climate models and satellite observations. *Atmospheric Chemistry and Physics*, *20*(22), 13835–13855.

Zelinka, M. D., Zhou, C., & Klein, S. A. (2016). Insights from a refined decomposition of cloud feedbacks. *Geophysical Research Letters*, *43*(17), 9259–9269.

Zhang, K., Zhang, W., Wan, H., Rasch, P. J., Ghan, S. J., Easter, R. C., ... others (2022). Effective radiative forcing of anthropogenic aerosols in e3sm version 1: historical changes, causality, decomposition, and parameterization sensitivities. *Atmospheric Chemistry and Physics*, *22*(13), 9129–9160.

Zhang, S., Zhang, K., Wan, H., & Sun, J. (2022). Further improvement and evaluation of nudging in the e3sm atmosphere model version 1 (eamv1). *Geoscientific Model Development Discussions*, 1–37.

Zhang, Y., Ye, A., Nguyen, P., Analui, B., Sorooshian, S., & Hsu, K. (2021). New insights into error decomposition for precipitation products. *Geophysical Research Letters*, *48*(17), e2021GL094092.

Zheng, G., Wang, Y., Aiken, A. C., Gallo, F., Jensen, M. P., Kollias, P., ... others (2018). Marine boundary layer aerosol in the eastern north atlantic: seasonal variations and key controlling processes. *Atmospheric Chemistry and Physics*, *18*(23), 17615–17635.